Development 138, 1717-1726 (2011) doi:10.1242/dev.059881

Arterial-venous network formation during brain vascularization involves hemodynamic regulation of chemokine signaling

Jeroen Bussmann[1], Scot A. Wolfe[2,3] and Arndt F. Siekmann[1,*]

SUMMARY

During angiogenic sprouting, newly forming blood vessels need to connect to the existing vasculature in order to establish a functional circulatory loop. Previous studies have implicated genetic pathways, such as VEGF and Notch signaling, in controlling angiogenesis. We show here that both pathways similarly act during vascularization of the zebrafish central nervous system. In addition, we find that chemokine signaling specifically controls arterial-venous network formation in the brain. Zebrafish mutants for the chemokine receptor *cxcr4a* or its ligand *cxcl12b* establish a decreased number of arterial-venous connections, leading to the formation of an unperfused and interconnected blood vessel network. We further find that expression of *cxcr4a* in newly forming brain capillaries is negatively regulated by blood flow. Accordingly, unperfused vessels continue to express *cxcr4a*, whereas connection of these vessels to the arterial circulation leads to rapid downregulation of *cxcr4a* expression and loss of angiogenic characteristics in endothelial cells, such as filopodia formation. Together, our findings indicate that hemodynamics, in addition to genetic pathways, influence vascular morphogenesis by regulating the expression of a proangiogenic factor that is necessary for the correct pathfinding of sprouting brain capillaries.

KEY WORDS: Zebrafish, Chemokine, Brain vasculature, Capillaries, Hemodynamics, Angiogenesis, Zinc-finger nuclease

INTRODUCTION

The formation of a functional circulatory network requires proper connections between the arterial and venous circulation. These connections are established during development via the formation of capillary beds situated between major arteries and veins. Failure to correctly pattern these capillary beds results in shunting between arteries and veins and can lead to arterial-venous malformations (Mullan et al., 1996). Work in recent years has shown that genetic cues, such as Sonic hedgehog, Vascular endothelial growth factor (VEGF) and Notch are essential for initial vascular patterning. Mouse embryos mutant for a single allele of *Vegfa* show severe vascular defects (Carmeliet et al., 1996; Ferrara et al., 1996). In the developing zebrafish trunk vasculature, reduction of VEGF signaling leads to a loss of arterial marker gene expression (Lawson et al., 2003; Lawson et al., 2002). Similar to VEGF signaling, Notch signaling is necessary for arterial differentiation both in mouse and zebrafish embryos (Duarte et al., 2004; Lawson et al., 2001; Zhong et al., 2001). Furthermore, VEGF signaling has been shown to act upstream of the Notch pathway during arterial differentiation (Lawson et al., 2002). A more recent report also suggests a direct involvement of the Hedgehog pathway in arterial differentiation (Williams et al., 2010). Thus, Sonic hedgehog, VEGF and Notch are necessary for proper arterial gene expression and the separation of arteries and veins. This genetic control of arterial differentiation is already in place during early embryonic stages, prior to the onset of circulation.

[1]Max-Planck Institute for Molecular Biomedicine, Roentgenstr. 20, 48149 Muenster, Germany. [2]Program in Gene Function and Expression, University of Massachusetts Medical School, Worcester, MA 01602, USA. [3]Department of Biochemistry and Molecular Pharmacology, University of Massachusetts Medical School, Worcester, MA 01602, USA.

*Author for correspondence (arndt.siekmann@mpi-muenster.mpg.de)

Accepted 17 February 2011

In contrast to their common role during arterial differentiation, VEGF and Notch signaling have opposing roles in controlling angiogenic sprouting. Whereas VEGF signaling promotes angiogenesis, Notch signaling negatively regulates angiogenic sprouting (Phng and Gerhardt, 2009). This regulation might in part be achieved via the negative regulation of VEGF receptor expression by Notch (Siekmann et al., 2008). Therefore, Notch signaling serves as an important node in controlling arterial differentiation and angiogenesis. After blood circulation starts, physiological feedback mechanisms further shape the vascular tree. These include tissue oxygenation, in addition to changes in hemodynamics (le Noble et al., 2008). Similar to the genetic pathways discussed above, studies in chick embryos have shown that changes in blood flow can influence arterial gene expression (le Noble et al., 2004). In addition, a recent report suggests that blood flow regulates the expression of a microRNA and thereby influences VEGF signaling within endothelial cells (Nicoli et al., 2010). Despite these insights, our understanding of how genetic pathways are integrated with hemodynamic cues during arterial-venous network formation remains limited.

Chemokines are a group of small vertebrate-specific proteins that were initially identified due to their role in controlling cell migration during the immune response (Luster, 1998). They bind to G protein-coupled seven-transmembrane receptors. Of these, Cxcr4 and its ligand Cxcl12 (Sdf-1) have received increasing attention because they also play a crucial role in guiding cell migration in diverse developmental contexts, such as germ cell and neuronal migration, melanophore patterning, muscle and heart formation and blood vessel development (Raz and Mahabaleshwar, 2009). We have previously shown that *cxcr4a* is important for the formation of the lateral dorsal aortae in zebrafish embryos (Siekmann et al., 2009). In later embryonic development, *Cxcr4* and *Cxcl12* play essential roles during the vascularization of specific organs in mouse embryos, such as the gastrointestinal tract

(Tachibana et al., 1998) and the kidneys (Takabatake et al., 2009). However, the mechanisms by which *cxcr4* influences vascular morphogenesis remain elusive.

Here, we have analyzed the mechanisms that control blood vessel formation in the hindbrain of zebrafish embryos. Our findings illustrate that, similar to other vascular beds, VEGF and Notch signaling control arterial gene expression and angiogenic sprouting of the hindbrain vasculature. We have also uncovered a specific role for chemokine signaling in the formation of the hindbrain capillary network. In zebrafish embryos that bear knockout alleles of the chemokine receptor *cxcr4a* or its ligand *cxcl12b*, hindbrain capillaries fail to establish proper links to the arterial circulation and show an increased number of unperfused interconnections that remain angiogenic. In addition, we show that angiogenic behaviors, such as the formation of filopodial extensions and the expression of *cxcr4a*, are negatively regulated by blood flow. Based on these results, we propose that changes in hemodynamics serve as a feedback mechanism that ensures the proper formation of arterial-venous connections and the establishment of a functional circulatory loop.

MATERIALS AND METHODS

Zebrafish strains and morpholinos

Zebrafish were maintained as described previously (Westerfield, 1993). Previously described zebrafish lines were *Tg(kdrl:egfp)*^{s843} (Jin et al., 2005), *Tg(kdrl:HRAS-mCherry)*^{s916} (Hogan et al., 2009), *Tg(fli1a:nEGFP)*^{y7} (Roman et al., 2002), *Tg(UAS:myc-Notch1a-intra)*^{kca3} (Scheer and Campos-Ortega, 1999), *Tg(UAS:GFP)*^{nkuasgfp1a} (Asakawa and Kawakami, 2008), *cxcr4a*^{um20} (Siekmann et al., 2009) and *kdrl*^{hu5088} (Bussmann et al., 2010). Morpholinos (MOs) targeting *cardiac troponin T2* (*tnnt2*) (2 ng/embryo) (Sehnert et al., 2002), *gata1* (8.4 ng/embryo) (Galloway et al., 2005), *dll4* (10 ng/embryo) (Siekmann and Lawson, 2007) and a standard control MO (2-10 ng/embryo) (Siekmann et al., 2009) have been described previously.

Generation of the *Tg(cdh5*^{BAC}*:gal4ff)*^{mu101} transgenic line

The construct to generate the *Tg(cdh5*^{BAC}*:gal4ff)*^{mu101} transgenic line was generated using Red/ET recombineering (GeneBridges). We used bacterial artificial chromosome (BAC) clone CH73-357K2, which contains 101.7 kb of the *cdh5* locus, including 33 kb upstream of the start codon and 57.9 kb downstream of the stop codon. In a first round of recombineering, an iTol2_ampR cassette (Suster et al., 2009) was inserted into the BAC vector backbone. The recombineering cassette was amplified from the iTol2_amp plasmid by PCR using primers pTARBAC_iTol2_fw (5′-gcgtaagcggggcacatttcattacctctttctccgcacccgacatagatCCCTGCTCGAGCC-GGGCCCAAGTG-3′) and pTarBAC_iTol2_rev (5′-gcggggcatgactattg-gcgcgccggatcgatccttaattaagtctactaATTATGATCCTCTAGATCAGATC-3′); homology to the BAC vector is depicted in lower case. In a second round of recombineering, a gal4ff_kanR cassette [modified from Suster et al. (Suster et al., 2009)] was inserted at the start codon of *cdh5*. This cassette was amplified from the pCS2+gal4ff_kanR plasmid using primers cdh5_HA1_gal4ff_fw (5′-ctacaaggcatgaattatcatacagatatttgttttgttgtttttctgc-agATGAAGCTACTGTCTTCTATCGAAC-3′) and cdh5_HA2_kanR_rev (5′-gcaaccctgaagacaggctcagtcatctgccttctggcacactgtttcatTCAGAAGAACT-CGTCAAGAAGGCG-3′). Recombineering was performed according to the manufacturer's protocol. BAC DNA was isolated by Midiprep (Invitrogen) and injected at 100 pg/embryo together with 25 pg/embryo of *tol2* transposase mRNA (Kawakami et al., 2004) into embryos heterozygous for *Tg(UAS:GFP)*. Embryos displaying endothelial-restricted expression were selected at 5 days post-fertilization (dpf) and grown to adulthood. Founders were identified through outcrossing. Four founder fish were identified out of seven adult fish screened; all lines displayed endothelial-restricted expression. The line driving highest GFP expression when crossed with UAS-GFP was used in this study. This line, *Tg(cdh5*^{BAC}*:gal4ff)*^{mu101}, was inherited as a single locus in a Mendelian fashion.

For Notch gain-of-function experiments, adult *Tg(cdh5*^{BAC}*:gal4ff)*^{mu101}, *Tg(UAS:GFP)*^{nkuasgfp1a} double-heterozygous fish were crossed with fish heterozygous for a myc-tagged zebrafish Notch1a intracellular domain (*NICD*) driven by the upstream activating sequence [*Tg(uas:myc-Notch1a-intra)*] (Scheer and Campos-Ortega, 1999). Using this crossing scheme, 50% of GFP-positive fish overexpressed *NICD* specifically in endothelial cells.

Generation of *cxcr4a*^{um21} and *cxcl12b*^{mu100} mutant zebrafish

Zinc-finger nucleases (ZFNs) against *cxcl12b* were designed as previously described (Siekmann et al., 2009). In the *cxcl12b*^{mu100} allele, 15 nt of wild-type (wt) *cxcl12b* exon 2 (5′-CCTCAACACCGTCCC-3′) are deleted at the ZFN cut site and 2 nt (5′-GA-3′) are inserted. This leads to a frameshift in the *cxcl12b* coding sequence after 37 amino acids and a stop codon 23 amino acids later.

A novel *cxcr4a* mutant allele (*cxcr4a*^{um21}) was generated using the same ZFNs as previously described (Siekmann et al., 2009). In this allele, 29 nt of wt *cxcr4a* exon 2 (5′-TGACAGACAAGTACCGTCTGCACCTCTCA-3′) are deleted at the ZFN cut site and 4 nt (5′-GGAG-3′) are inserted. This leads to a frameshift in the *cxcr4a* coding sequence after 79 amino acids and a stop codon 32 amino acids later. The generation and identification of mutant alleles were carried out as described previously (Meng et al., 2008).

Genotyping

Primers used for genotyping *Tg(uas:myc-Notch1a-intra)* were described previously (Scheer and Campos-Ortega, 1999). Primers for genotyping *Tg(cdh5:gal4ff)*^{mu101} were cdh5_FWD (5′-ACAGTGTGTTTGCAT-CATTG-3′) and gal4FF_REV (5′-AGTAGCGACACTCCCAGTTG-3′), which gives a product of 350 bp. Primers for genotyping *kdrl*^{hu5088} were kdrl_FWD (5′-TGCCGATTGCAGATTATG-3′) and kdrl_REV (5′-CTC-ACCATCAATAGTCAAAGC-3′). PCR products were digested with *Dde*I (NEB). Fragment sizes are 402 bp for the *kdrl*^{WT} allele and 239 bp + 163 bp for the *kdrl*^{hu5088} allele.

Primers for genotyping *cxcl12b* were cxcl12b FWD (5′-AAGCC-CATCAGTCTGGTGGAGAGG-3′) and cxcl12b_REV (5′-GTGCC-CTTTGTCTGGTGTAACCTG-3′). PCR products were digested with *Taa*I (Fermentas). Fragment sizes are 51 bp + 124 bp for the *cxcl12b*^{WT} allele and 162 bp for the *cxcl12b*^{mu100} allele.

Primers for genotyping *cxcr4a* were cxcr4a FWD (5′-CCAAC-TTTGAGGTCCCGTGTGATG-3′) and cxcr4a_REV (5′-TCCAAACT-GATGAAGGCGAGGATG-3′). PCR products were digested with *Dde*I (NEB). Fragment sizes are 178 bp + 157 bp for the *cxcr4a*^{WT} allele and 310 bp for the *cxcr4a*^{um21} allele.

In situ hybridization, drug treatments and imaging

Whole-mount in situ hybridization was performed as previously described for single and two probe hybridization (Julich et al., 2005; Thisse and Thisse, 2008). Previously described probes were for *flt4*, *kdrl* (Lawson et al., 2001), *dab2* (Covassin, L. et al., 2006), *flt1* (Bussmann et al., 2007), *dll4* (Siekmann and Lawson, 2007), *cxcr4a* (Siekmann et al., 2009), *vegfaa* (Lawson et al., 2002) and *vegfab* (Bahary et al., 2007).

Micro-angiography was performed as previously described (Nicoli et al., 2010). For in vivo imaging, live embryos were mounted in 0.5% low melting point agarose in E3 medium containing 84 mg/l tricaine (0.5×; 168 mg/l being the standard dose for zebrafish anesthesia) to inhibit movement and 0.003% phenylthiourea to inhibit pigmentation. Confocal image stacks were collected on an SP5 confocal microscope (inverted) with a 20× objective (Leica Microsystems) and processed using Imaris 3D visualization software (Bitplane) and ImageJ (NIH).

To inhibit blood flow, stock solutions of 4 g/l tricaine in 20 mM Tris buffer (pH 7.2) (Nicoli et al., 2010) or 10 mM nifedipine (Sigma-Aldrich) in dimethylsulfoxide (DMSO) (Langheinrich et al., 2003) were diluted in E3 medium containing 0.003% phenylthiourea. Embryos were incubated for 1 hour and then fixed in 4% paraformaldehyde. For washout experiments, embryos were washed once with E3 buffer, and then transferred to E3 medium without tricaine.

In order to inhibit Notch signaling, embryos were treated with 50 μM N-[N-(3,5-difluorophenacetyl-L-alanyl)]-S-phenylglycine t-butyl ester (DAPT). Control embryos were treated with 0.2% DMSO.

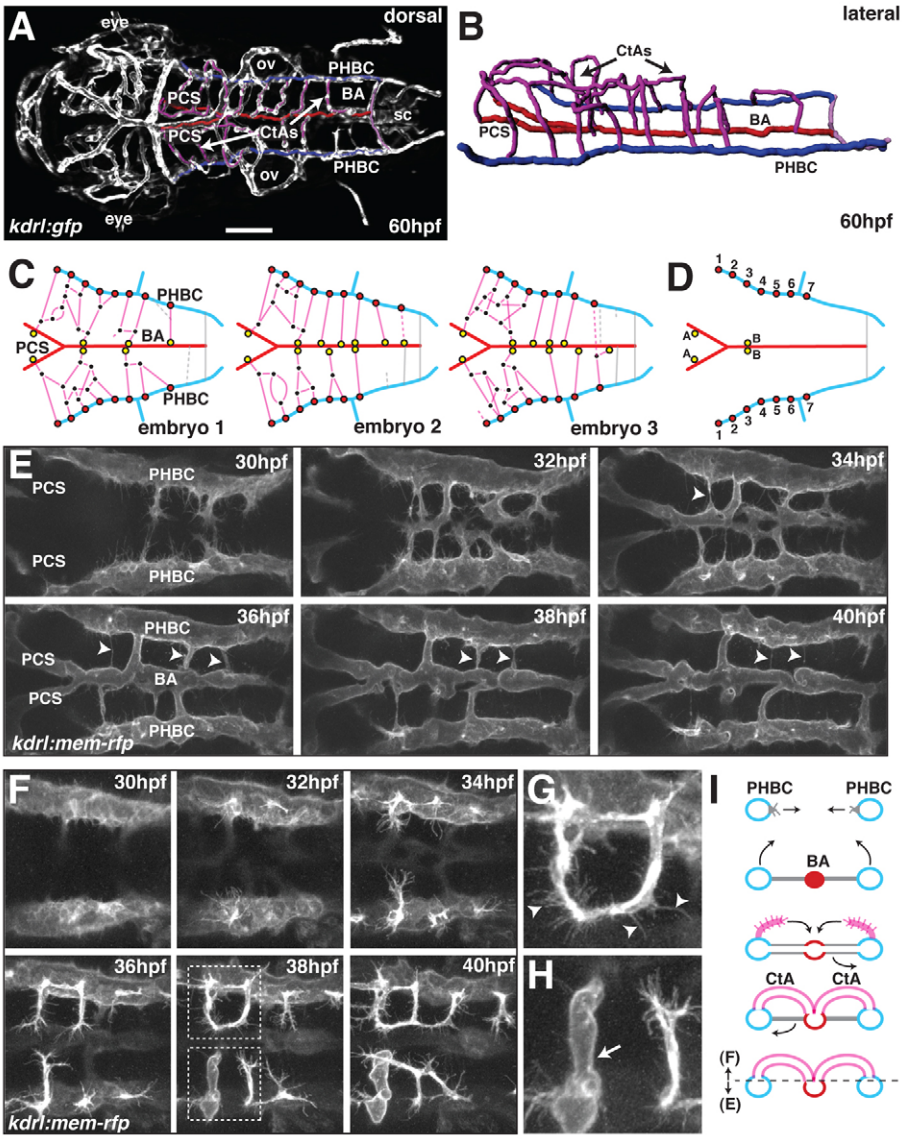

Fig. 1. Development of the zebrafish hindbrain vasculature. (**A**) Maximal intensity projection of a confocal *z*-stack of a *kdrl:gfp* transgenic zebrafish brain at 60 hpf, indicating the position of the primordial hindbrain channels (PHBCs, blue), posterior communicating segments (PCSs, red), basilar artery (BA, red) and central arteries (CtAs, magenta). Dorsal view, anterior to the left. ov, otic vesicle; sc, spinal cord. Scale bar: 100 μm (**B**) Wire diagram of the hindbrain vasculature based on angiography at 60 hpf. Lateral oblique view. Color coding as in A. (**C**) Schematic representation of the hindbrain vascular network at 60 hpf in three individual wild-type (wt) embryos based on confocal *z*-stacks of *kdrl:gfp* transgenic embryos, indicating the position of PHBC-CtA connections (red filled circles), CtA-CtA connections (black dots) and CtA-BA/PCS connections (yellow filled circles). Dashed lines indicate connections without a visible lumen. Gray lines represent ventral (non-CtA) connections between the PHBC and the BA. (**D**) Schematic representation of stereotyped vascular connections in the hindbrain vascular network at 60 hpf. A and B, fixed CtA to BA connections; C, fixed PHBC to CtA connections. (**E**) Confocal time-lapse of BA formation in live *kdrl:mem-rfp* transgenic embryos between 30 and 40 hpf. Arrowheads indicate pruning of ventral non-CtA connections between the PHBC and the BA. (**F-H**) Confocal time-lapse of CtA formation in live *kdrl:mem-rfp* transgenic embryos. The boxed regions are enlarged in G and H, showing the presence of filopodial extensions on a non-lumenized CtA (arrowheads, G) but not on a lumenized CtA (arrow, H). (**I**) Schematic representation of BA and CtA formation. Transverse view. The dashed line indicates the planar level at which E and F were separated.

Quantification of hindbrain connectivity was performed on confocal *z*-stacks of *kdrl:mem-rfp* transgenic or *kdrl:mem-rfp, fli1a:nuc-gfp* double-transgenic embryos using Imaris 3D. Cell numbers were quantified in the PHBC (rostral of the connection to the mid-cerebral vein to the most caudal connection with the BA), the hindbrain CtAs and the BA (rostral of the branchpoint with the PCSs to the most caudal connection with the PHBC). For quantification, we assembled individual *z*-stacks in Imaris 3D and used single *z*-planes to determine endothelial cell numbers. For total cell numbers, these values were summed and the number of cells in direct (ventral) BA to PHBC connections was added. The Mann-Whitney non-parametric test as implemented in SPSS Statistics 19 (IBM) was used to analyze the data.

RESULTS

Dynamic visualization of the forming hindbrain vasculature

At 60 hours post-fertilization (hpf), the hindbrain vasculature consists of a centrally located basilar artery (BA), which is connected to the bilateral primordial hindbrain channels (PHBCs) on both sides of the hindbrain by arch-shaped brain capillaries, called the central arteries (CtAs). These either connect directly from the PHBC to the BA or interconnect before fusing to the BA (Fig. 1A,B, arrows). At its most anterior point, the BA is connected bilaterally to the arterial circulation via the posterior communicating segments (PCSs), as previously shown by angiography (Isogai et al., 2001). When comparing different wild-type (wt) embryos, we noticed that the number and position of CtA sprouts from the PHBCs are stereotyped (Fig. 1C,D, red filled circles), similar to previous observations concerning the development of the early blood vessels in the trunk (Isogai et al., 2003). In contrast to this, CtA connections exhibited considerable variation among embryos. Connections to the BA were generally fewer in number and randomized in their positions (Fig. 1C,D, yellow filled circles). This was partially due to a variable number of interconnections between individual CtAs (Fig. 1C, red lines connecting black circles). The exceptions were two connections with the PCS and two connections in the anterior part of the BA, which always occurred at the same position. In addition, a ventral connection between the PHBCs and the BA always linked the PHBCs to the posterior BA (Fig. 1C,D, gray lines). Thus, whereas the venous connections of the CtAs are stereotyped, arterial connections of the CtAs to the BA appear partially stochastic.

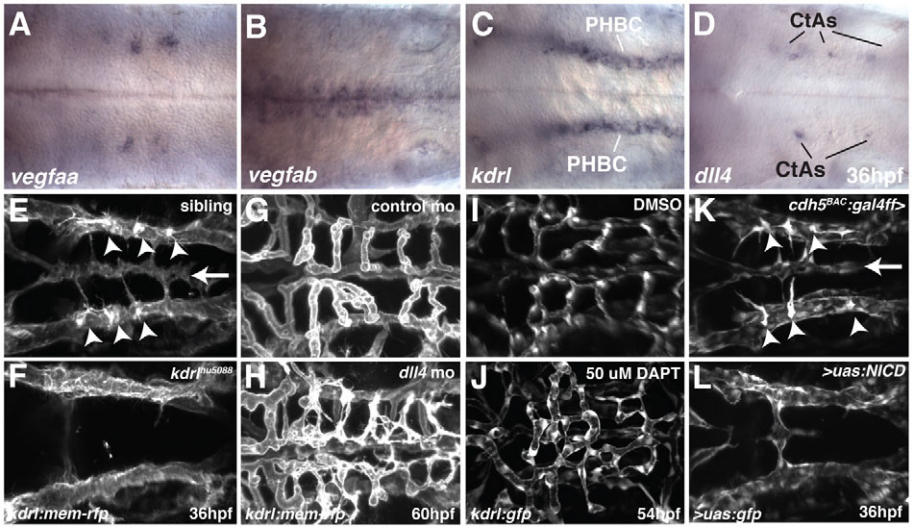

Fig. 2. VegfA and Notch signaling are required for angiogenic sprouting in the zebrafish hindbrain. (**A-D**) Whole-mount in situ hybridization showing the expression of *vegfaa* (A), *vegfab* (B), *kdrl* (C) and *dll4* (D) at 36 hpf. (**E-L**) Maximal intensity projections of confocal *z*-stacks at 36 (E,F,K,L), 54 (I,J) or 60 (G,H) hpf. Arrowheads indicate CtA sprouts emerging from the PHBC. Arrow indicates the position of the BA. (E,F) Sibling (E) or *kdrl* mutant (F) embryos, with endothelial cells labeled by *kdrl:mem-rfp* expression. (G,H) *kdrl:mem-rfp*-expressing embryos injected with control MO (G) or *dll4* MO (H). (I,J) *kdrl:gfp*-expressing embryos treated from 30 to 54 hpf with DMSO (I) or DAPT (J). (K,L) Embryos from a cross between *cdh5:gal4ff, uas:gfp* and *uas:NICD*. The embryo in K is negative for *uas:NICD*, whereas that in L is heterozygous for *uas:NICD*. Endothelial cells are labeled by *cdh5:gal4ff, uas:gfp* expression. Dorsal views, anterior to the left.

In order to better understand the processes leading to these variations within the hindbrain vasculature, we performed confocal time-lapse imaging in *kdrl:mem-rfp* transgenic embryos (see Movies 1-3 in the supplementary material). Our dynamic visualization revealed that the arterial part of the hindbrain vasculature forms by two waves of angiogenic sprouting originating from the PHBCs (Fig. 1E,F; see Movie 1 in the supplementary material). An initial wave between 30 and 40 hpf forms the ventrally located BA, resulting in a triad of blood vessels with a centrally located artery and bilateral veins (Fig. 1E,I; see Movie 2 in the supplementary material). This initial wave leaves ventral interconnections between the BA and the PHBC, most of which are later pruned. At its caudal end, two of these ventral connections persist. At its rostral end, the BA connects to the anterior arterial circulation by fusing to the bilateral PCSs. Shortly after the first wave, angiogenic blood vessel sprouts emanate from both PHBCs and migrate dorsomedially (Fig. 1F,I; see Movie 3 in the supplementary material). Here, they either anastomose (Fig. 1F, 38 hours, upper boxed area; see also Fig. 1G) or continue to migrate ventromedially, ultimately connecting to the BA (Fig. 1F, 38 hours, lower boxed area, see also Fig. 1H). We noticed that connection of a CtA sprout to the BA leads to the rapid downregulation of filopodial extensions on the respective sprout and to the formation of a visible lumen within the sprout (Fig. 1H, arrow). These changes in cellular morphology could occur within 10 minutes (see Fig. S1 and Movie 4 in the supplementary material). By contrast, an anastomosis between two unperfused sprouting CtAs did not lead to the loss of filopodial extensions or to the appearance of a clearly visible lumen (Fig. 1G, arrowheads). If one of the anastomosing CtAs was previously perfused through connection to the BA, then the anastomosis led to a rapid loss of filopodia and to the appearance of a visible lumen in the unperfused CtA sprout. Therefore, CtA sprouts only ceased to display angiogenic characteristics upon connecting to a perfused target blood vessel, either directly to the BA or indirectly to the BA through a perfused CtA.

Arterial-venous gene expression patterns during angiogenic sprouting of the hindbrain vasculature

The initial stereotypical sprouting of CtAs from the PHBCs resembles the sprouting pattern of intersegmental arteries in the zebrafish trunk (Isogai et al., 2003). Previous work has identified the VEGF and Notch signaling pathways as important for the formation of these blood vessels (Covassin, L. D. et al., 2006; Leslie et al., 2007; Siekmann and Lawson, 2007). We therefore reasoned that the same genetic pathways might regulate sprouting of the hindbrain capillaries. To address this, we performed in situ hybridization for VEGF and Notch signaling pathway components. The zebrafish genome contains two VegfA ligands, VegfAa and VegfAb (Bahary et al., 2007). At 36 hpf, we detected expression of VegfAa in distinct stripes within the hindbrain, where CtAs emerge (Fig. 2A). VegfAb was expressed in midline cells, including the cephalic floor plate (Fig. 2B), at a position directly dorsal to the forming BA. We detected mRNA of the VegfA receptor *kdrl* in all endothelial cells (Fig. 2C; see Fig. S2A-C in the supplementary material). In addition, the Notch ligand *dll4* was expressed in sprouting CtAs (Fig. 2D; see Fig. S2D-F in the supplementary material). Thus, VegfA ligands and their receptor and the Notch ligand *dll4* were expressed during the formation of the hindbrain vasculature.

A more detailed analysis of arterial and venous markers revealed expression of the venous markers *dab2* (Covassin, L. et al., 2006) and *flt4* (Lawson et al., 2001) in cells of the PHBC at 28 hpf (see Fig. S2G-L in the supplementary material). These findings are in agreement with the previous characterization of the PHBC as the major head vein (Isogai et al., 2001). However, we noted lower expression levels of *dab2* in the region adjacent to the otic vesicles

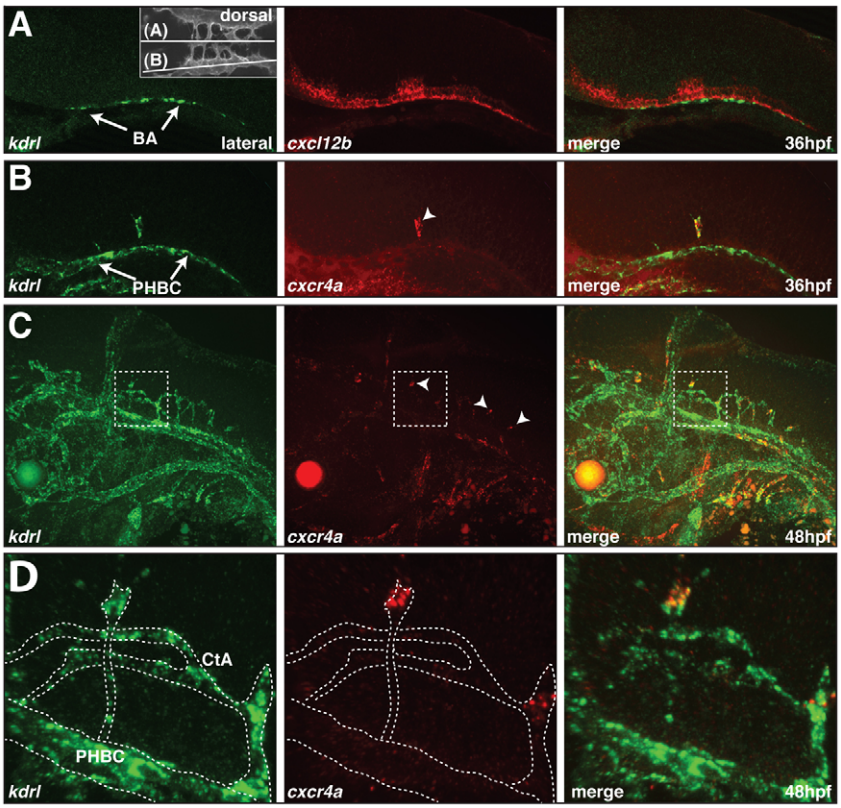

Fig. 3. Expression of *cxcl12b* and *cxcr4a* in the zebrafish hindbrain. (**A-D**) Two-color fluorescent in situ hybridization showing the distribution of *kdrl* mRNA (green) and *cxcl12b* (A) and *cxcr4a* (B-D) mRNA (red). Lateral views, anterior to the left. (A) *cxcl12b* and *kdrl* expression at 36 hpf. Inset indicates the plane of view in A and B. (B) *cxcr4a* and *kdrl* expression at 36 hpf. Arrowhead indicates a single *cxcr4a*-expressing CtA sprout. (C) *cxcr4a* and *kdrl* expression at 48 hpf. Arrowheads indicate tip cells of CtA sprouts expressing *cxcr4a*. (D) Enlargement of the boxed area in C. The *kdrl*-positive endothelial cells are outlined.

at 28 hpf. This became more pronounced at the 36 hpf time point. We observed a similar downregulation in *flt4* expression at 36 hpf. However, weak *flt4* expression could be detected in sprouting CtA cells (see Fig. S2L in the supplementary material). In addition to *dll4*, we also detected expression of *flt1*, another arterial marker in zebrafish (Bussmann et al., 2007), in sprouting CtAs (see Fig. S2M-O in the supplementary material). We could not detect *dll4* or *flt1* expression at 28 hpf in cells of the PHBC (Fig. S2D,M in the supplementary material). However, both genes were induced shortly thereafter. At 36 hpf, *dll4* and *flt1* were expressed in a subset of PHBC endothelial cells and in sprouting CtAs (see Fig. S2F,O in the supplementary material). We furthermore detected the expression of these genes in the BA (see Fig. S2N in the supplementary material). Thus, the onset of CtA sprouting was characterized by a downregulation of venous marker genes in parts of the PHBC, while arterial markers started to be expressed (see Fig. S2S-U in the supplementary material).

VEGF and Notch signaling control sprouting of the hindbrain vasculature

Based on our gene expression analysis, we reasoned that VEGF and Notch signaling might be involved in regulating hindbrain angiogenesis. To address this, we analyzed the effects of VEGF and Notch gain and loss of function on the formation of the hindbrain vasculature. Zebrafish embryos mutant for VEGF receptor 2 (*kdrl*^{hu5088}) (Bussmann et al., 2010) showed normal head circulation and PHBC formation at 36 hpf. However, whereas wt siblings showed normal BA and CtA sprout formation (Fig. 2E), both vessel types were missing in mutant embryos (Fig. 2F). In *kdrl* ^{hu5088} mutant embryos, *dll4* and *flt1* expression was absent from the PHBC, indicating that induction of arterial gene expression is VegfA-dependent (see Fig. S3A-D in the supplementary material). Downregulation of *dab2* and *flt4* in the PHBC was found to be independent of *kdrl* (see Fig. S3E,F in the supplementary material; data not shown). Loss of the BA and CtA sprouts persisted until at least 60 hpf, at which time the PHBCs contained a higher number of endothelial cells in *kdrl* mutants than in the wt. The total endothelial cell number in the hindbrain vasculature was lower in *kdrl* mutants (see Fig. S4A-C in the supplementary material), suggesting that the migration and proliferation of endothelial cells both contributed to hindbrain blood vessel formation. Thus, VegfA signaling selectively influences the formation of the arterial vasculature in the hindbrain, similar to previous observations in the zebrafish trunk (Lawson et al., 2003). As VegfA-mediated angiogenesis is antagonized by Notch signaling in the trunk (Leslie et al., 2007; Siekmann and Lawson, 2007), we asked whether Notch signaling might play the same role during hindbrain vascularization. Inactivation of the Notch signaling pathway via morpholino (MO) knockdown of the Notch ligand Dll4 led to an increase in CtA interconnections at 60 hpf (Fig. 2G,H; see Fig. S4 in the supplementary material). A similar phenotype was observed in embryos treated with the γ-secretase inhibitor DAPT, which inhibits the activation of Notch receptors (Fig. 2I,J). Both treatments led to a reduction of arterial marker gene expression, including that of *dll4* and *flt1*, in CtA endothelial cells (see Fig. S3G-N in the supplementary material).

In order to activate the Notch signaling pathway in all endothelial cells, we used a two-component transgenic system that leads to the expression of the constitutively active Notch intracellular domain (NICD) in all endothelial cells (see Materials and methods). Double-transgenic embryos showed a delay of BA sprouting and a strong reduction of CtA sprouting (Fig. 2K,L). Furthermore, endothelial cell numbers were decreased in double-transgenic embryos (see Fig. S4G-I in the supplementary material). Thus, inactivation of the Notch signaling pathway causes an increase in angiogenic sprouting, whereas Notch pathway

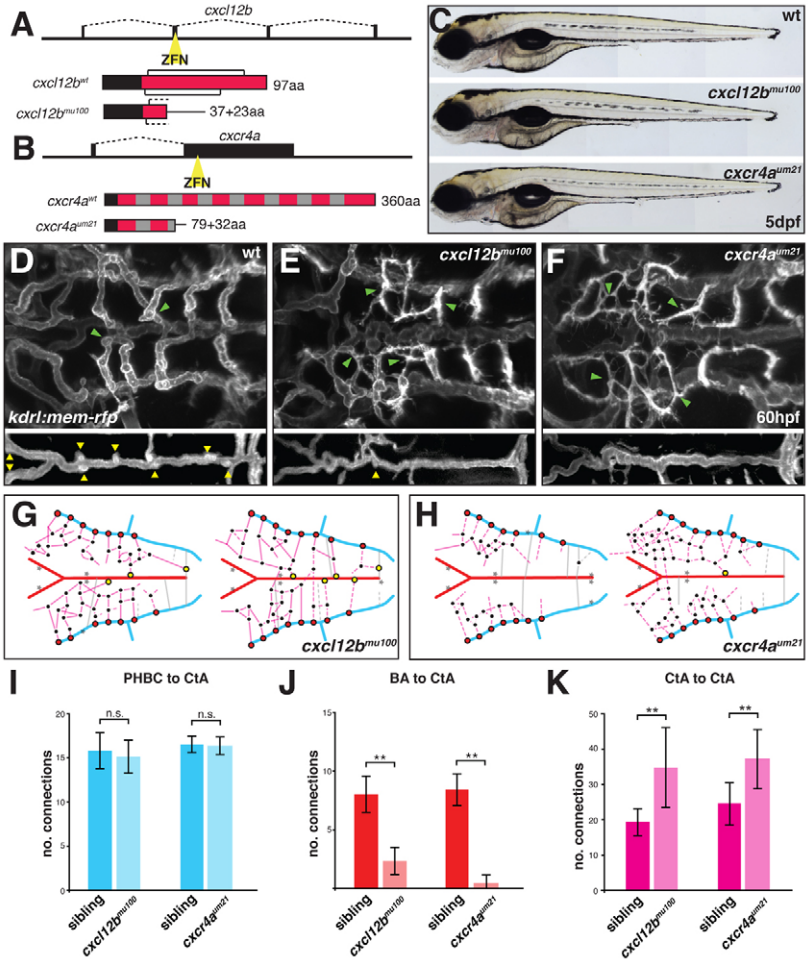

Fig. 4. *cxcl12b* and *cxcr4a* are required for hindbrain vascular patterning. (**A**,**B**) Schematic representation of *cxcl12b* (A) and *cxcr4a* (B) mutant generation using zinc-finger nucleases (ZFNs). Black boxes in the gene structure represent exons and dashed lines represent introns. Yellow triangle indicates the position of the ZFN targeting site. Protein structures are displayed as red boxes. Black brackets indicate the position of conserved cysteine bridges for Cxcl12b. Black boxes in the protein structure represent the signal peptide for secretion (Cxcl12b) or membrane targeting (Cxcr4a). Gray boxes indicate the position of transmembrane helices for Cxcr4a. aa, amino acid. (**C**) Brightfield images of wt, *cxcl12b*^{mu100} and *cxcr4a*^{um21} homozygous mutant zebrafish at 5 dpf. (**D-F**) Maximal intensity projections of confocal *z*-stacks of *kdrl:mem-rfp* transgenic embryos at 60 hpf. wt (D), *cxcl12b*^{mu100} (E) and *cxcr4a*^{um21} (F) homozygous mutants are shown. Yellow arrowheads indicate CtA to BA connections; green arrowheads indicate CtA to CtA connections. (**G**,**H**) Schematic representation of the hindbrain vascular network in two individual *cxcl12b* ^{mu100} (G) and *cxcr4a*^{um21} (H) homozygous mutant embryos based on confocal *z*-stacks of *kdrl:gfp* transgenic embryos. Color coding as in Fig. 1C. Gray stars indicate missing conserved vascular connections. (**I-K**) Quantitative analysis of hindbrain patterning in wt, *cxcl12b*^{mu100} and *cxcr4a*^{um21} homozygous mutant zebrafish. Vessel connections were counted from confocal *z*-stacks of *kdrl:gfp* transgenic embryos. **, $P<0.05$; n.s., not significant (Mann-Whitney U test). $n=6$ embryos per group. Error bars represent s.d.

activation inhibits angiogenesis. Gene expression analysis showed that *dab2* and *flt4* were also downregulated in the anterior PHBC in embryos overexpressing NICD (see Fig. S3O,P in the supplementary material; data not shown). By contrast, the arterial makers *dll4* and *flt1* were ectopically expressed throughout the PHBC in these embryos (see Fig. S3Q-T in the supplementary material).

Expression of *cxcl12b* and its receptor *cxcr4a* during hindbrain blood vessel development

In order to identify additional genes that might play a role during the formation of the hindbrain vasculature, we examined the expression patterns of factors implicated in the directed migration of endothelial cells. Double fluorescent in situ hybridization revealed expression of the chemokine *cxcl12b* in a stripe along the midline of the neural keel, immediately above the BA at 36 hpf (Fig. 3A; see Movie 5 in the supplementary material). This restricted expression pattern of *cxcl12b* suggested that chemokine signaling might play a role during hindbrain capillary sprouting. Accordingly, we found expression of *cxcr4a*, the known receptor for *cxcl12b*, in the tips of sprouting CtAs at 36 hpf (Fig. 3B, arrowhead; see Fig. S2P,R in the supplementary material) and transiently in the BA (see Fig. S2Q in the supplementary material). This tip cell restriction of *cxcr4a* expression was also found at 48 hpf (Fig. 3C,D, arrowheads; see Movie 6 in the supplementary material). At this time point, CtAs in the anterior part of the hindbrain that had connected to the BA no longer showed *cxcr4a* expression. Therefore, *cxcr4a* is specifically expressed in the tips of migrating CtAs and is downregulated upon their connection to the BA.

Chemokine signaling through *cxcr4a* is important for establishing the arterial-venous connections of hindbrain capillaries

In order to investigate the function of chemokine signaling during the formation of the hindbrain vasculature, we generated loss-of-function alleles for *cxcl12b* and *cxcr4a* using zinc-finger nucleases (Fig. 4A,B; see Materials and methods). Homozygous mutant embryos of both lines appeared phenotypically normal at 5 dpf (Fig. 4C) and were viable and fertile in adulthood. Phenotypic comparison of the previously described lateral dorsal aorta (LDA) phenotype for *cxcr4a*^{um20} mutants, which carries an in-frame five amino acid deletion in the second transmembrane domain (Siekmann et al., 2009), revealed that LDA formation was also affected in *cxcr4a*^{um21} and *cxcl12*^{mu100} mutants at 24 hpf. However, in contrast to the fully penetrant phenotype of both alleles of *cxcr4a*, fewer than 50% of *cxcl12b* mutants showed defects in LDA formation (see Table S1 in the supplementary material), suggesting that compensatory mechanisms exist to guide the migration of LDA cells in *cxcl12b* mutants.

We next analyzed the formation of the hindbrain vasculature in *cxcl12b*^{mu100} and *cxcr4a*^{um21} mutants at 60 hpf. At this stage, anterior CtAs in wt embryos were connected to the BA (Fig. 4D, yellow arrowheads in inset). In addition, we detected several

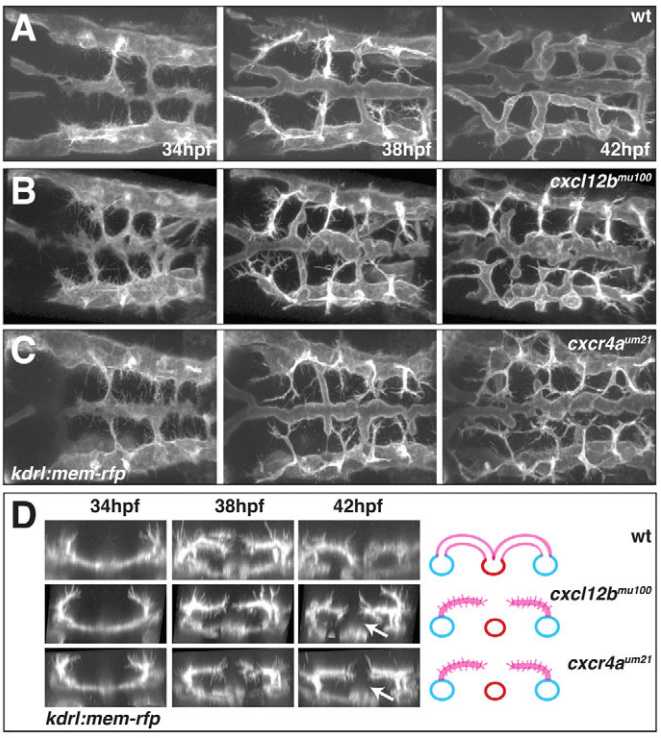

Fig. 5. Time-lapse imaging of hindbrain vascular development in wt, *cxcl12b*^{mu100} and *cxcr4a*^{um21} mutant embryos. (**A-C**) Still images at 34, 38 and 42 hpf from confocal time-lapse movies of hindbrain vascular development in live wt (A), *cxcl12b*^{mu100} (B) and *cxcr4a*^{um21} (C) mutant *kdrl:mem-rfp* transgenic embryos (see Movies 7-9 in the supplementary material). Dorsal views, anterior to the left. (**D**) Transverse sections based on 3D reconstruction of the movies illustrated in A-C, highlighting the absence of ventral migration of CtA sprouts in *cxcl12b*^{mu100} and *cxcr4a*^{um21} mutant embryos (arrows). The schematic interpretations are based on 42 hpf still images as in Fig. 1I.

interconnections between CtAs (Fig. 4D, green arrowheads; see also Fig. 1C). Embryos mutant for either *cxcl12b* (Fig. 4E,G) or *cxcr4a* (Fig. 4F,H) showed no change in the number or position of initial CtA sprouts (Fig. 4I). Endothelial cell numbers were also normal in both mutants (see Fig. S5 in the supplementary material). However, the number of connections between CtAs and the BA was greatly reduced (Fig. 4E,F, yellow arrowheads in insets; Fig. 4G,H, yellow circles; compare with Fig. 1C,D and Fig. 4J for quantification). We never detected connections between CtAs and the BA at the four fixed positions present in wt embryos. At the same time, the number of CtA interconnections increased (Fig. 4K). Therefore, the stochastic event of CtAs connecting to the BA was selectively affected in *cxcl12b*^{mu100} and *cxcr4a*^{um21} mutants, leading to an increase in CtA interconnections. Interestingly, we also observed an increase in filopodial extensions emanating from the CtAs of mutant embryos, which resembles an earlier, angiogenic time point during CtA formation in wt embryos (compare Fig. 4E,F with Fig. 1G).

To understand the hindbrain vascular phenotypes in *cxcl12b*^{mu100} and *cxcr4a*^{um21} in more detail, we performed confocal time-lapse imaging of *kdrl:mem-rfp* transgenic embryos followed by 3D reconstruction (Fig. 5; see Movies 7-12 in the supplementary material). This analysis revealed that the initial migration of PHBC endothelial cells to the midline occurred normally in both mutant strains, although the BA occasionally appeared misshapen (Fig. 5A-C). Initial CtA sprouting from the PHBCs was also normal. However, after their initial dorsomedial migration, CtA sprouts failed to migrate ventrally towards the BA (Fig. 5D, arrows). These results indicate that the observed phenotypes in hindbrain vascular connectivity in *cxcl12b*^{mu100} and *cxcr4a*^{um21} are likely to result from defects in CtA migration, starting between 38 and 42 hpf.

In contrast to the observed defects in the hindbrain vasculature, formation of the trunk vasculature was unaffected in *cxcl12b*^{um100} and *cxcr4a*^{um21} mutants (data not shown), similar to previous observations for a different *cxcr4a* allele (Siekmann et al., 2009). Thus, whereas Notch and VEGF signaling affect angiogenesis in both the trunk and the brain, chemokine signaling specifically affects hindbrain angiogenesis.

Establishment of functional arterial-venous connections leads to loss of angiogenic properties in sprouting hindbrain capillaries

Based on our observations that CtA perfusion led to a rapid loss of angiogenic properties, such as filopodial extensions (Fig. 1H), we hypothesized that endothelial gene expression profiles might similarly change upon the establishment of functional CtA-BA connections. In order to affect the perfusion of CtAs, we exposed embryos to a sublethal dose of tricaine, which was previously used to inhibit blood flow in zebrafish embryos (Nicoli et al., 2010). These treatments slowed down the heart rate without stopping circulation. In contrast to control embryos, in which CtAs were perfused at 52 hpf (Fig. 6A), we found a variable number of unperfused CtAs in treated embryos. These unperfused CtAs displayed an increased number of filopodial extensions (Fig. 6B, arrowheads). This indicates that lowering the blood flow and thereby perfusion of CtAs led to an increase in angiogenic activity, similar to the observed cell behavior in *cxcl12b*^{mu100} and *cxcr4a*^{um21} mutants. A previous report showed that blood flow could negatively influence *cxcr4a* expression in the zebrafish trunk (Packham et al., 2009). Consistently, we found a dose-dependent increase of *cxcr4a* expression in CtAs after 1 hour of tricaine treatment (Fig. 6C-E; see Fig. S6A-E,G in the supplementary material). To exclude direct effects of tricaine on *cxcr4a* regulation, we used a second drug (nifedipine) to inhibit blood flow. This treatment similarly led to an increase in *cxcr4a* expression (see Fig. S6F in the supplementary material). In order to determine whether this increase in *cxcr4a* expression was reversible by re-establishing circulation in CtAs, we performed washout experiments (see Fig. S6H-P in the supplementary material). Removal of tricaine led to a partial downregulation of *cxcr4a* expression after 75 minutes and complete downregulation after 150 minutes. Embryos continuously treated with tricaine for the same periods of time did not show a downregulation of *cxcr4a* expression. This indicates that re-establishing circulation in CtAs can lead to the downregulation of *cxcr4a* expression.

Consistent with the loss of CtA perfusion, we observed a similar upregulation of *cxcr4a* expression in both *cxcl12b*^{mu100} and *cxcr4a*^{um21} mutants (Fig. 6F,G). In addition, embryos injected with an MO targeting the *tnnt2* gene, which never establish circulation, also displayed *cxcr4a* upregulation (Fig. 6H). More detailed analysis using two-color double in situ hybridization with probes for *kdrl* and *cxcr4a* established a specific upregulation of *cxcr4a* in arterial endothelial cells in these embryos (Fig. 6I, compare with Fig. 3C). These observations suggest that the onset of blood flow in CtA sprouts leads to the rapid downregulation of *cxcr4a*

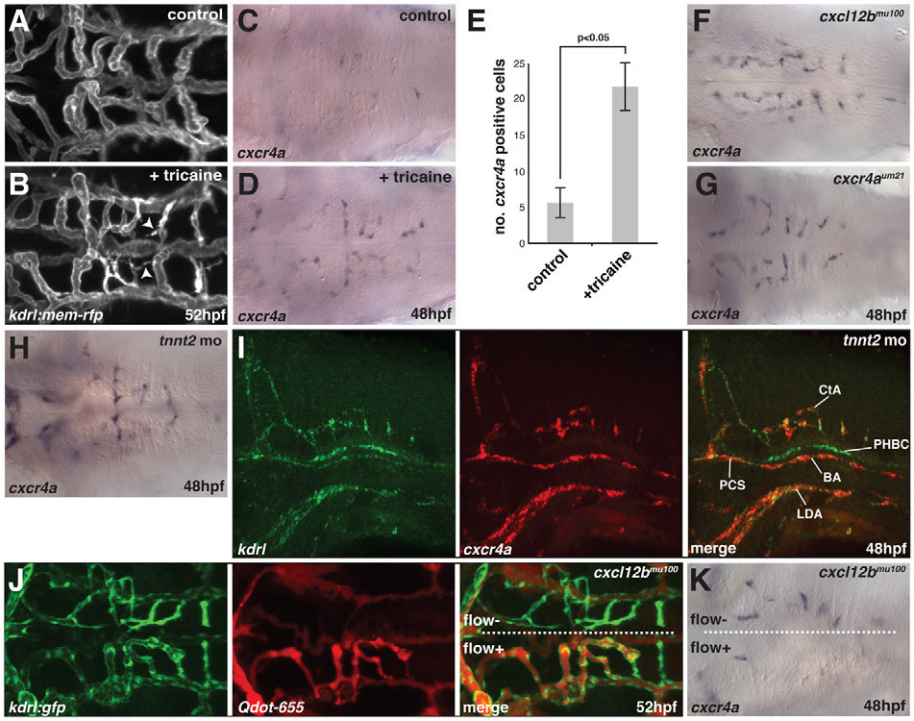

Fig. 6. Flow is required for hindbrain vascular patterning and downregulation of *cxcr4a* expression. (**A**,**B**) Maximal intensity projections of confocal *z*-stacks of *kdrl:mem-rfp* transgenic zebrafish embryos at 52 hpf, untreated (A) or treated for 8 hours with 2× tricaine (B). Arrowheads indicate the presence of filopodia on non-perfused CtAs. (**C**,**D**) In situ hybridization for *cxcr4a* mRNA in untreated control embryos fixed at 48 hpf (C) or embryos treated for 1 hour with 2× tricaine from 47-48 hpf and fixed at 48 hpf (D). (**E**) Quantitative analysis of *cxcr4a* mRNA expression. *cxcr4a*-expressing cells were counted in embryos following *cxcr4a* in situ hybridization. $P<0.05$ (Mann-Whitney U test). $n=15$ embryos per group. Error bars represent s.d. (**F-H**) *cxcr4a* in situ hybridization in *cxcl12b*^{mu100} (F) and *cxcr4a*^{um21} (G) homozygous mutant embryos or embryos injected with 2 ng *tnnt2* MO at the 1-cell stage (H) and fixed at 48 hpf. (**I**) Two-color fluorescent in situ hybridization of embryos injected with 2 ng *tnnt2* MO and fixed at 48 hpf, showing the distribution *cxcr4a* mRNA (red) and *kdrl* mRNA (green). (**J**) Angiography using Quantum dots (Qdot-655; Invitrogen) in a *kdrl:gfp* transgenic, *cxcl12b*^{mu100} homozygous mutant embryo at 52 hpf. In this embryo, only one half of the brain had perfused CtAs (flow+ versus flow–). (**K**) In situ hybridization for *cxcr4a* mRNA in a *cxcl12b*^{mu100} homozygous mutant embryo in which half of the hindbrain contained perfused CtAs at 48 hpf. Dorsal views, anterior to the left, except in I, which is a side view with anterior to the left.

expression. Therefore, changes in the functional status of a sprouting capillary could lead to changes in endothelial gene expression.

To further explore this, we analyzed *Tg(kdrl:egfp)*^{s843}*; cxcl12b*^{um100} embryos in which capillaries were only perfused on one side of the brain (Fig. 6J; see Movie 13 in the supplementary material). Angiography in these embryos revealed the presence of individual CtA connections to the BA on the perfused side, whereas an interconnected network of hindbrain capillaries was present on the unperfused side. In these mutants, *cxcr4a* was strongly expressed in unperfused vessels, whereas the side containing perfused CtAs showed weaker levels of *cxcr4a* expression (Fig. 6K), similar to what we observed in wt embryos. Thus, perfusion of CtAs in *cxcl12b*^{mu100} embryos led to downregulation of *cxcr4a* expression. Interestingly, *cxcr4a*^{um21} mutants did not develop perfused CtAs until after 60 hpf (see Fig. S7 in the supplementary material). These findings also indicate that the observed upregulation of *cxcr4a* in *cxcl12b*^{mu100} and *cxcr4a*^{um21} embryos is not due to a negative-feedback loop, in which *cxcr4a* signaling would downregulate its own expression. Together, these results suggest that perfusion of CtAs leads to a downregulation of *cxcr4a* expression and to the cessation of angiogenic activity.

Perfusion of a given blood vessel might affect endothelial cells in several ways. Shear stress has been shown to influence the organization of the cytoskeleton and to initiate downstream signaling events (Hahn and Schwartz, 2009). In addition, blood flow through a vessel would provide the tissue with oxygen, repressing hypoxia-regulated signal transduction pathways (Fraisl et al., 2009). In order to differentiate between these possibilities, we injected zebrafish embryos with an MO targeting *gata1* (Galloway et al., 2005). These embryos were severely anemic at 36 hpf owing to a block in erythrocyte differentiation (see Fig. S8A,B in the supplementary material). We examined the morphology of the hindbrain vasculature in these embryos at 50 hpf and found no difference between *gata1* MO-injected and control MO-injected embryos (see Fig. S8C,D in the supplementary material). In addition, we did not detect a change in *cxcr4a* expression in these embryos (see Fig. S8E,F in the supplementary material). Therefore, the observed effect on the morphology of CtA endothelial cells and the downregulation of *cxcr4a* expression are most likely mediated via the effects of increased plasma shear stress on endothelial cells.

DISCUSSION

We have used in vivo time-lapse imaging to analyze the formation of the hindbrain capillaries in developing zebrafish embryos. Our results show that the arterial network of the brain is largely derived from pre-existing veins via angiogenic sprouting. Whereas the number and position of initial venous sprouts are stereotyped and well defined along the anterior-posterior axis, the connections of these sprouts to the arterial circulation are highly variable. These

observations suggest that genetic cues initially determine the position of venous sprouts. The later-occurring connections of these sprouts to the arterial circulation appear to be stochastic. Our time-lapse movies reveal that endothelial tip cells of the sprouting CtAs can form connections with other CtA tip cells or with the BA, leading to different outcomes with respect to cellular morphology and sprouting behavior. Connection to the BA results in the rapid downregulation of angiogenic properties, such as filopodia formation, whereas interconnected CtAs remain angiogenic. Since it is not predetermined which CtAs interconnect, these observations can explain the stochastic nature of CtA-BA connections.

The formation of the trunk vasculature is directed by a number of genetic cues. Whereas VEGF signaling provides a pro-angiogenic cue, Notch signaling has been shown to negatively regulate angiogenesis (Covassin, L. D. et al., 2006; Leslie et al., 2007; Siekmann and Lawson, 2007). Our analysis now reveals that the same molecules orchestrate the formation of the brain arterial vasculature. In this setting, the absence of VEGF signaling or activation of the Notch signaling pathway lead to a loss of BA and CtA sprouting. Conversely, downregulation of Notch signaling increases angiogenic sprouting in both vascular beds. These findings illustrate that the signaling molecules are conserved among sprouting trunk and brain vessels as well as their antagonistic relationship. Therefore, the VEGF and Notch signaling pathways are reiteratively used during embryonic blood vessel development. It is of interest to note that mutants for *cxcr4* or *cxcl12b* do not show any phenotypes during the sprouting of intersomitic vessels in the zebrafish trunk, but do affect angiogenesis in the brain. These findings indicate that different genetic pathways are used to guide endothelial migration in distinct vascular beds. A possible explanation for this might be differences in the connections that sprouting cells need to make in a given anatomical location. In the trunk, intersegmental arteries migrate dorsally, where they fuse to form the dorsal longitudinal anastomosing vessel (DLAV). Initially, these vessels comprise a closed arterial loop without connections to the venous circulation. Venous connections are subsequently established via a second wave of angiogenic sprouts from the ventrally located vein, transforming ~50% of intersegmental arteries into veins (Isogai et al., 2003). By contrast, sprouting hindbrain vessels need to connect to the medially located BA in order to close the circulatory loop. This process is selectively affected in mutants for *cxcr4a* or *cxcl12b*. Thus, different guidance cues are activated in distinct sets of endothelial cells in order to meet distinct anatomical requirements.

Several recent reports have illustrated the influence of hemodynamics on the developing vasculature, including the formation of the aortic arches in mice (Yashiro et al., 2007) and zebrafish (Nicoli et al., 2010) and the remodeling of the yolk vasculature in chicken (Buschmann et al., 2010) and mouse (Lucitti et al., 2007). However, little is known about the integration of hemodynamic stimuli with genetic pathways and, in particular, the functional relevance of this interaction. Our results reveal that *cxcr4a* expression is high in unperfused capillary sprouts that have not connected to their final target blood vessel – in this case, the BA. Expression of *cxcr4a* is not influenced by CtA anastomoses, as the termination of CtA angiogenesis at this step would lead to the establishment of non-productive venous loops. Therefore, maintaining high levels of *cxcr4a* in unperfused vessels ensures the proper pathfinding of sprouting capillaries towards the arterial circulation. Upon connecting to the arterial network, perfusion of capillaries occurs, leading to rapid changes of cell morphology. As documented in our time-lapse movies, these changes occur in less than 10 minutes. Our results furthermore show that gene expression patterns change upon vessel perfusion. For instance, expression of *cxcr4a* mRNA is rapidly downregulated. Thus, receiving input from the arterial circulation provides sprouting endothelial cells with a hemodynamic stimulus that results in the downregulation of angiogenic properties.

Previous reports have highlighted the role of genetic pathways in this process. For instance, the Notch signaling pathway has been shown to negatively influence angiogenic sprouting via regulation of VEGF receptor levels (Siekmann et al., 2008). However, our observations suggest a rapid response in endothelial cells upon perfusion. Therefore, a fast hemodynamic stimulus might initiate the downregulation of the angiogenic program in parallel with genetic factors. We observed that the establishment of a single functional BA connection in *cxcl12b*^{mu100} mutants led to the perfusion of the entire capillary network on the respective side of the brain. This indicates that the observed CtA interconnections in *cxcr4a*^{um21} and *cxcl12b*^{mu100} mutants can resolve into a functional vascular network upon connecting to the arterial circulation. This is in contrast to the vascular phenotypes observed in Notch loss-of-function mutants, in which endothelial cells form a similar interconnected network (Gridley, 2007). In this setting, the vasculature fails to be perfused. It remains to be determined which mechanisms account for these differences in vascular function in the two classes of mutant.

Our findings, together with a report from Fujita et al. (Fujita et al., 2011), are the first to demonstrate a role of chemokine signaling in the formation of the brain vasculature. Recent reports have highlighted the function of *cxcr4* and *cxcl12* in the formation of organ-specific vascular beds (Tachibana et al., 1998; Takabatake et al., 2009). In the developing gut mesenteries, interconnections between the superior mesenteric artery and the venous circulation are greatly reduced in mice lacking *cxcr4* function (Ara et al., 2005). In addition, treating neonate mice with an inhibitor of Cxcr4 leads to the formation of long angiogenic sprouts without interconnections in the developing retinal vasculature (Strasser et al., 2010). Furthermore, collateral vessel formation in zebrafish depends on Cxcr4a signaling (Packham et al., 2009). These reports suggest that our findings concerning the function of *cxcr4* during the guided migration of venous-derived angiogenic sprouts towards the arterial circulation might be conserved between different species and capillary beds. Together, our findings illustrate how a hemodynamic feedback loop can control endothelial gene expression and thereby ensure the formation of proper arterial-venous connections within a newly forming capillary bed.

Acknowledgements

We thank Nathan Lawson and Friedemann Kiefer for critical reading of the manuscript; Brant Weinstein for sharing data before publication; Reinhild Bussmann for excellent fish care; and Frauke Vaque for technical assistance. This work was funded by the Max Planck Society and an ERC starting grant (260794-ZebrafishAngio) awarded to A.F.S. J.B. was supported by a long-term EMBO post-doctoral fellowship. S.A.W. was supported by a grant from the National Heart, Lung, and Blood Institute of the NIH (1R01HL093766 to S.A.W. and Nathan D. Lawson). Deposited in PMC for release after 12 months.

Competing interests statement

The authors declare no competing financial interests.

Supplementary material

Supplementary material for this article is available at
http://dev.biologists.org/lookup/suppl/doi:10.1242/dev.059881/-/DC1

References

Ara, T., Tokoyoda, K., Okamoto, R., Koni, P. A. and Nagasawa, T. (2005). The role of CXCL12 in the organ-specific process of artery formation. *Blood* **105**, 3155-3161.

Asakawa, K. and Kawakami, K. (2008). Targeted gene expression by the Gal4-UAS system in zebrafish. *Dev. Growth Differ.* **50**, 391-399.

Bahary, N., Goishi, K., Stuckenholz, C., Weber, G., Leblanc, J., Schafer, C. A., Berman, S. S., Klagsbrun, M. and Zon, L. I. (2007). Duplicate VegfA genes and orthologues of the KDR receptor tyrosine kinase family mediate vascular development in the zebrafish. *Blood* **110**, 3627-3636.

Buschmann, I., Pries, A., Styp-Rekowska, B., Hillmeister, P., Loufrani, L., Henrion, D., Shi, Y., Duelsner, A., Hoefer, I., Gatzke, N. et al. (2010). Pulsatile shear and Gja5 modulate arterial identity and remodeling events during flow-driven arteriogenesis. *Development* **137**, 2187-2196.

Bussmann, J., Bakkers, J. and Schulte-Merker, S. (2007). Early endocardial morphogenesis requires Scl/Tal1. *PLoS Genet.* **3**, e140.

Bussmann, J., Bos, F. L., Urasaki, A., Kawakami, K., Duckers, H. J. and Schulte-Merker, S. (2010). Arteries provide essential guidance cues for lymphatic endothelial cells in the zebrafish trunk. *Development* **137**, 2653-2657.

Carmeliet, P., Ferreira, V., Breier, G., Pollefeyt, S., Kieckens, L., Gertsenstein, M., Fahrig, M., Vandenhoeck, A., Harpal, K., Eberhardt, C. et al. (1996). Abnormal blood vessel development and lethality in embryos lacking a single VEGF allele. *Nature* **380**, 435-439.

Covassin, L., Amigo, J. D., Suzuki, K., Teplyuk, V., Straubhaar, J. and Lawson, N. D. (2006). Global analysis of hematopoietic and vascular endothelial gene expression by tissue specific microarray profiling in zebrafish. *Dev. Biol.* **299**, 551-562.

Covassin, L. D., Villefranc, J. A., Kacergis, M. C., Weinstein, B. M. and Lawson, N. D. (2006). Distinct genetic interactions between multiple Vegf receptors are required for development of different blood vessel types in zebrafish. *Proc. Natl. Acad. Sci. USA* **103**, 6554-6559.

Duarte, A., Hirashima, M., Benedito, R., Trindade, A., Diniz, P., Bekman, E., Costa, L., Henrique, D. and Rossant, J. (2004). Dosage-sensitive requirement for mouse Dll4 in artery development. *Genes Dev.* **18**, 2474-2478.

Ferrara, N., Carver-Moore, K., Chen, H., Dowd, M., Lu, L., O'Shea, K. S., Powell-Braxton, L., Hillan, K. J. and Moore, M. W. (1996). Heterozygous embryonic lethality induced by targeted inactivation of the VEGF gene. *Nature* **380**, 439-442.

Fraisl, P., Mazzone, M., Schmidt, T. and Carmeliet, P. (2009). Regulation of angiogenesis by oxygen and metabolism. *Dev. Cell* **16**, 167-179.

Fujita, M., Cha, Y. R., Pham, V. N., Sakurai, A., Roman, B. L., Gutkind, J. S. and Weinstein, B. M. (2011). Assembly and patterning of the vascular network of the vertebrate hindbrain. *Development* **138**, 1705-1715.

Galloway, J. L., Wingert, R. A., Thisse, C., Thisse, B. and Zon, L. I. (2005). Loss of gata1 but not gata2 converts erythropoiesis to myelopoiesis in zebrafish embryos. *Dev. Cell* **8**, 109-116.

Gridley, T. (2007). Notch signaling in vascular development and physiology. *Development* **134**, 2709-2718.

Hahn, C. and Schwartz, M. A. (2009). Mechanotransduction in vascular physiology and atherogenesis. *Nat. Rev. Mol. Cell Biol.* **10**, 53-62.

Hogan, B. M., Bos, F. L., Bussmann, J., Witte, M., Chi, N. C., Duckers, H. J. and Schulte-Merker, S. (2009). Ccbe1 is required for embryonic lymphangiogenesis and venous sprouting. *Nat. Genet.* **41**, 396-398.

Isogai, S., Horiguchi, M. and Weinstein, B. M. (2001). The vascular anatomy of the developing zebrafish: an atlas of embryonic and early larval development. *Dev. Biol.* **230**, 278-301.

Isogai, S., Lawson, N. D., Torrealday, S., Horiguchi, M. and Weinstein, B. M. (2003). Angiogenic network formation in the developing vertebrate trunk. *Development* **130**, 5281-5290.

Jin, S. W., Beis, D., Mitchell, T., Chen, J. N. and Stainier, D. Y. (2005). Cellular and molecular analyses of vascular tube and lumen formation in zebrafish. *Development* **132**, 5199-5209.

Julich, D., Hwee Lim, C., Round, J., Nicolaije, C., Schroeder, J., Davies, A., Geisler, R., Lewis, J., Jiang, Y. J. and Holley, S. A. (2005). beamter/deltaC and the role of Notch ligands in the zebrafish somite segmentation, hindbrain neurogenesis and hypochord differentiation. *Dev. Biol.* **286**, 391-404.

Kawakami, K., Takeda, H., Kawakami, N., Kobayashi, M., Matsuda, N. and Mishina, M. (2004). A transposon-mediated gene trap approach identifies developmentally regulated genes in zebrafish. *Dev. Cell* **7**, 133-144.

Langheinrich, U., Vacun, G. and Wagner, T. (2003). Zebrafish embryos express an orthologue of HERG and are sensitive toward a range of QT-prolonging drugs inducing severe arrhythmia. *Toxicol. Appl. Pharmacol.* **193**, 370-382.

Lawson, N. D., Scheer, N., Pham, V. N., Kim, C. H., Chitnis, A. B., Campos-Ortega, J. A. and Weinstein, B. M. (2001). Notch signaling is required for arterial-venous differentiation during embryonic vascular development. *Development* **128**, 3675-3683.

Lawson, N. D., Vogel, A. M. and Weinstein, B. M. (2002). sonic hedgehog and vascular endothelial growth factor act upstream of the Notch pathway during arterial endothelial differentiation. *Dev. Cell* **3**, 127-136.

Lawson, N. D., Mugford, J. W., Diamond, B. A. and Weinstein, B. M. (2003). phospholipase C gamma-1 is required downstream of vascular endothelial growth factor during arterial development. *Genes Dev.* **17**, 1346-1351.

le Noble, F., Moyon, D., Pardanaud, L., Yuan, L., Djonov, V., Matthijsen, R., Breant, C., Fleury, V. and Eichmann, A. (2004). Flow regulates arterial-venous differentiation in the chick embryo yolk sac. *Development* **131**, 361-375.

le Noble, F., Klein, C., Tintu, A., Pries, A. and Buschmann, I. (2008). Neural guidance molecules, tip cells, and mechanical factors in vascular development. *Cardiovasc. Res.* **78**, 232-241.

Leslie, J. D., Ariza-McNaughton, L., Bermange, A. L., McAdow, R., Johnson, S. L. and Lewis, J. (2007). Endothelial signalling by the Notch ligand Delta-like 4 restricts angiogenesis. *Development* **134**, 839-844.

Lucitti, J. L., Jones, E. A., Huang, C., Chen, J., Fraser, S. E. and Dickinson, M. E. (2007). Vascular remodeling of the mouse yolk sac requires hemodynamic force. *Development* **134**, 3317-3326.

Luster, A. D. (1998). Chemokines – chemotactic cytokines that mediate inflammation. *N. Engl. J. Med.* **338**, 436-445.

Meng, X., Noyes, M. B., Zhu, L. J., Lawson, N. D. and Wolfe, S. A. (2008). Targeted gene inactivation in zebrafish using engineered zinc-finger nucleases. *Nat. Biotechnol.* **26**, 695-701.

Mullan, S., Mojtahedi, S., Johnson, D. L. and Macdonald, R. L. (1996). Embryological basis of some aspects of cerebral vascular fistulas and malformations. *J. Neurosurg.* **85**, 1-8.

Nicoli, S., Standley, C., Walker, P., Hurlstone, A., Fogarty, K. E. and Lawson, N. D. (2010). MicroRNA-mediated integration of haemodynamics and Vegf signalling during angiogenesis. *Nature* **464**, 1196-1200.

Packham, I. M., Gray, C., Heath, P. R., Hellewell, P. G., Ingham, P. W., Crossman, D. C., Milo, M. and Chico, T. J. (2009). Microarray profiling reveals CXCR4a is downregulated by blood flow in vivo and mediates collateral formation in zebrafish embryos. *Physiol. Genomics* **38**, 319-327.

Phng, L. K. and Gerhardt, H. (2009). Angiogenesis: a team effort coordinated by notch. *Dev. Cell* **16**, 196-208.

Raz, E. and Mahabaleshwar, H. (2009). Chemokine signaling in embryonic cell migration: a fisheye view. *Development* **136**, 1223-1229.

Roman, B. L., Pham, V. N., Lawson, N. D., Kulik, M., Childs, S., Lekven, A. C., Garrity, D. M., Moon, R. T., Fishman, M. C., Lechleider, R. J. et al. (2002). Disruption of acvrl1 increases endothelial cell number in zebrafish cranial vessels. *Development* **129**, 3009-3019.

Scheer, N. and Campos-Ortega, J. A. (1999). Use of the Gal4-UAS technique for targeted gene expression in the zebrafish. *Mech. Dev.* **80**, 153-158.

Sehnert, A. J., Huq, A., Weinstein, B. M., Walker, C., Fishman, M. and Stainier, D. Y. (2002). Cardiac troponin T is essential in sarcomere assembly and cardiac contractility. *Nat. Genet.* **31**, 106-110.

Siekmann, A. F. and Lawson, N. D. (2007). Notch signalling limits angiogenic cell behaviour in developing zebrafish arteries. *Nature* **445**, 781-784.

Siekmann, A. F., Covassin, L. and Lawson, N. D. (2008). Modulation of VEGF signalling output by the Notch pathway. *BioEssays* **30**, 303-313.

Siekmann, A. F., Standley, C., Fogarty, K. E., Wolfe, S. A. and Lawson, N. D. (2009). Chemokine signaling guides regional patterning of the first embryonic artery. *Genes Dev.* **23**, 2272-2277.

Strasser, G. A., Kaminker, J. S. and Tessier-Lavigne, M. (2010). Microarray analysis of retinal endothelial tip cells identifies CXCR4 as a mediator of tip cell morphology and branching. *Blood* **115**, 5102-5110.

Suster, M. L., Sumiyama, K. and Kawakami, K. (2009). Transposon-mediated BAC transgenesis in zebrafish and mice. *BMC Genomics* **10**, 477.

Tachibana, K., Hirota, S., Iizasa, H., Yoshida, H., Kawabata, K., Kataoka, Y., Kitamura, Y., Matsushima, K., Yoshida, N., Nishikawa, S. et al. (1998). The chemokine receptor CXCR4 is essential for vascularization of the gastrointestinal tract. *Nature* **393**, 591-594.

Takabatake, Y., Sugiyama, T., Kohara, H., Matsusaka, T., Kurihara, H., Koni, P. A., Nagasawa, Y., Hamano, T., Matsui, I., Kawada, N. et al. (2009). The CXCL12 (SDF-1)/CXCR4 axis is essential for the development of renal vasculature. *J. Am. Soc. Nephrol.* **20**, 1714-1723.

Thisse, C. and Thisse, B. (2008). High-resolution in situ hybridization to whole-mount zebrafish embryos. *Nat. Protoc.* **3**, 59-69.

Westerfield, M. (1993). *The Zebrafish Book*. Eugene, OR: University of Oregon Press.

Williams, C., Kim, S. H., Ni, T. T., Mitchell, L., Ro, H., Penn, J. S., Baldwin, S. H., Solnica-Krezel, L. and Zhong, T. P. (2010). Hedgehog signaling induces arterial endothelial cell formation by repressing venous cell fate. *Dev. Biol.* **341**, 196-204.

Yashiro, K., Shiratori, H. and Hamada, H. (2007). Haemodynamics determined by a genetic programme govern asymmetric development of the aortic arch. *Nature* **450**, 285-288.

Zhong, T. P., Childs, S., Leu, J. P. and Fishman, M. C. (2001). Gridlock signalling pathway fashions the first embryonic artery. *Nature* **414**, 216-220.